Chinese Chemical Letters 37 (2026) 111283

Contents lists available at ScienceDirect

Chinese Chemical Letters

journal homepage: www.elsevier.com/locate/cclet

Rational structure-based design and optimization of next-generation biphenyl-piperidine-triazine derivatives as potent non-nucleoside reverse transcriptase inhibitors

Kun Zhang[a,c,d,1], Li-Min Zhao[c,d,1], Tianhao Xing[a,c,d], Yueyue Bu[a,c,d], Qingyun Wang[a,c,d], Christophe Pannecouque[e], Erik De Clercq[e], Angela Corona[f], Laura Dettori[f], Enzo Tramontano[f], Shuai Wang[b,c,d,*], Fen-Er Chen[a,c,d,*]

[a] Institute of Pharmaceutical Research and School of Pharmaceutical Sciences, Zhengzhou University, Zhengzhou 450001, China
[b] State Key Laboratory of Natural and Biomimetic Drugs, Peking University, Beijing 100191, China
[c] Department of Chemistry, Engineering Center of Catalysis and Synthesis for Chiral Molecules, Fudan University, Shanghai 200433, China
[d] Shanghai Engineering Center of Industrial Asymmetric Catalysis for Chiral Drugs, Shanghai 200433, China
[e] Laboratory of Virology and Chemotherapy, Rega Institute for Medical Research, KU Leuven, Leuven B-3000, Belgium
[f] Department of Life and Environmental Sciences, University of Cagliari, Monserrato I-09042, Italy

ARTICLE INFO

Article history:
Received 5 March 2025
Revised 29 April 2025
Accepted 30 April 2025
Available online 21 May 2025

Keywords:
AIDS
HIV-1
NNRTIs
Biphenyl-piperidine-triazines
Anti-resistance efficacy

ABSTRACT

To enhance the anti-resistance efficacy of our previously disclosed naphthyl-triazine **5**, structure-based drug design strategy was rationally conducted to design a series of novel biphenyl-piperidine-triazine-containing non-nucleoside reverse transcriptase inhibitors. Remarkably, several of these compounds demonstrated single-digit nanomolar antiviral potency against both wild-type (WT) human immunodeficiency virus-1 (HIV-1) and five clinically relevant mutant strains. Among these, compound **11s** emerged as the most potent inhibitor, showing remarkable efficacy against WT HIV-1 (50 % effective concentration (EC_{50}) = 2 nmol/L) and five mutant strains (EC_{50} = 0.003–0.073 μmol/L), which was significantly superior to that of compound **5**. This optimized derivative demonstrated substantially improved pharmacological properties compared to existing drugs etravirine (ETR) and rilpivirine (RPV), showing a 4-fold reduction in cytotoxicity alongside 6-fold enhancement in selectivity index (50 % cytotoxic concentration (CC_{50}) = 19.69 μmol/L, selectivity index (SI) = 7438). The compound's metabolic profile revealed exceptional stability, with an elimination half-life ($t_{1/2}$ = 41.4 min) more than double that of RPV ($t_{1/2}$ = 16.03 min). Comprehensive safety evaluation indicated minimal cytochrome P450 (CYP) enzymes interference, low cardiac ion channel activity, and no observable acute toxicity, collectively suggesting a reduced risk profile for therapeutic applications. These promising characteristics significantly advance the development potential of biphenyl-piperidine-triazine derivatives as next-generation non-nucleoside reverse transcriptase inhibitors (NNRTIs), offering enhanced efficacy, improved safety, and favorable pharmacokinetic properties for antiretroviral therapy.

© 2025 Published by Elsevier B.V. on behalf of Chinese Chemical Society and Institute of Materia Medica, Chinese Academy of Medical Sciences.

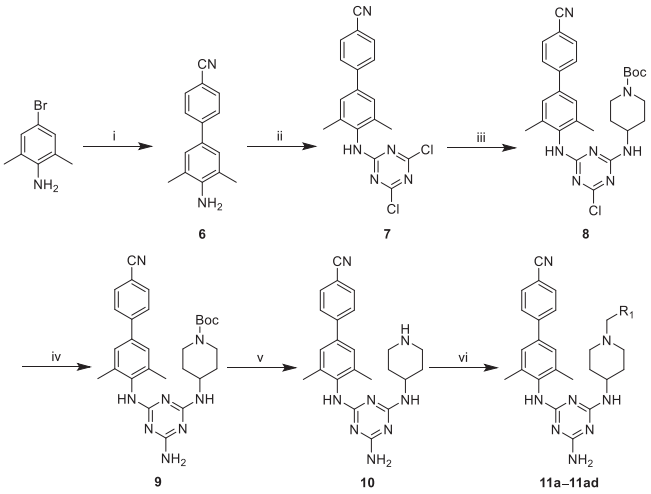
As one of the major global epidemic diseases, acquired immunodeficiency syndrome (AIDS) caused by human immunodeficiency virus (HIV) infection is a persistent threat to human health [1,2]. Reverse transcriptase (RT) is a key enzyme in HIV life cycle, which is responsible for the reverse transcription of single-stranded RNA into double-stranded DNA [3–5]. Non-nucleoside reverse transcriptase inhibitors (NNRTIs) are an important component of active antiviral therapy (ART) and widely applied in the treatment of AIDS [6–9]. Although ART has achieved remarkable success in suppressing HIV to undetectable levels, the virus cannot be eradicated and patients require lifelong ART administration [2,10,11]. Moreover, it has been reported that some NNRTIs have side effects and poor oral pharmacokinetic parameters [12–15]. Worst of all, the continuous emergence of resistant strains further limits the clinical effectiveness of these drugs [16–18]. Therefore, the discovery of novel NNRTIs that feature low toxicity, high efficiency, and anti-resistance activity is still urgent.

* Corresponding authors.
E-mail addresses: shuaiwang@fudan.edu.cn (S. Wang), rfchen@fudan.edu.cn (F.-E. Chen).
[1] These authors contributed equally to this work.

https://doi.org/10.1016/j.cclet.2025.111283
1001-8417/© 2025 Published by Elsevier B.V. on behalf of Chinese Chemical Society and Institute of Materia Medica, Chinese Academy of Medical Sciences.

In 2001, Janssen and co-workers reported the discovery of a triazine-containing NNRTI, namely compound **1**. This compound exhibited potent inhibitory activity against HIV-1 (50 % effective concentration (EC_{50}) = 0.0063 μmol/L, Fig. 1A) [19]. Over the subsequent decades, several series of optimizations and structural modifications based on compound **1** were carried out for a continuous and in-depth exploration [20–26]. Compound **2** was acquired through the modification of the linker and the aromatic ring at the C-4 position of triazine. It demonstrated potent inhibitory activity against HIV-1 (EC_{50} = 0.001 μmol/L). Nevertheless, its activity against the Y188L mutant strain declined sharply (EC_{50} = 0.124 μmol/L). Subsequently, by targeting the entrance channel of the non-nucleoside reverse transcriptase inhibitor binding pocket (NNIBP) and modifying the C-6 position of triazine, compound **3** was discovered (EC_{50} = 0.0078 μmol/L) [27]. To enhance the π-π stacking interactions between the ligand and the highly conserved hydrophobic region (W229), the phenyl group was substituted with a naphthyl moiety, affording compound **4**. This compound exhibited moderate anti-HIV-1 activity (EC_{50} = 34 nmol/L) along with low cytotoxicity (50 % cytotoxic concentration (CC_{50}) = 220 μmol/L) [28]. Removal of the allyl group yielded compound **5**, which had enhanced antiviral activity (EC_{50} = 9.4 nmol/L) against the wild-type (WT) HIV-1 [29]. Nonetheless, this analog showed unsatisfactory activity against mutant strains [30–32]. Thus, the development of novel triazine-based derivatives with increased antiviral activity against both WT and mutant strains continues to be a critical priority.

Analysis of the molecular modeling investigation indicated that compound **5** adopted a "horseshoe-shaped" conformation within the binding pocket (Fig. 1B). The β-naphthyl fragment occupied the hydrophobic area and formed multiple π-H interactions with W229 and a π-π interaction with Y181. The triazine core and the NH at the C-2 position formed two key hydrogen bonds with E138 and K101 respectively, and the NH_2 group formed an extra hydrogen bond with E138. The *p*-cyanophenyl group in the solvent-protein region did not interact with surrounding amino acids. To enhance the anti-resistance efficacy, a series of novel biphenyl-piperidine-triazine derivatives were designed and evaluated for their anti-HIV-1 activity. First, the β-naphthyl fragment was replaced with the biphenyl fragment to enhance hydrophobic interactions and π-π stacking length with surrounding residues. Then, a hydrophilic piperidyl moiety was introduced into the right wing to replace the *p*-cyanophenyl group, aiming to strengthen the interaction of the ligand with the solvent-protein region.



Scheme 1. Reagents and conditions: (i) 4-cyanophenylboronic acid, Pd(dppf)Cl_2, Cs_2CO_3, 1,4-dioxane:H_2O = 2:1, N_2, reflux, 12 h; (ii) cyanuric chloride, K_2CO_3, 1,4-dioxane, r.t., 2 h; (iii) 4-amino-1-Boc-piperidine, K_2CO_3, 1,4-dioxane, r.t., 3 h; (iv) $NH_3{\cdot}H_2O$, tetrahydrofuran (THF), 100 °C, 12 h; (v) CF_3COOH (TFA), dichloromethane (DCM), r.t., 0.5 h; (vi) corresponding benzyl bromide or chloride, K_2CO_3, *N*,*N*-dimethylformamide (DMF), r.t., 2–6 h.

The synthetic routes of **11a**–**11ad** are illustrated in Scheme 1. Specially, 4-bromo-2,6-dimethylaniline was chosen as starting material, and biphenyl fragment (**6**) was synthesized *via* Suzuki reaction [33,34]. Subsequently, **6** reacted with cyanuric chloride to generate **7**. This intermediate was then treated with 4-amino-1-Boc-piperidine to yield **8**. Then, an excess of $NH_3{\cdot}H_2O$ was employed to replace Cl atom in a sealed tube at 100 °C, and intermediate **9** was gained after 12 h. Following this, **10** was synthesized by deprotecting the Boc group [35,36]. Finally, **11a**–**11ad** were obtained *via* the nucleophilic substitution reaction.

The antiviral activity and cytotoxicity of the triazine derivatives **11a**–**11ad** were assessed in MT-4 cell cultures infected with the WT HIV-1 IIIB strain, utilizing the testing method we have previously described [37]. The detailed data provided in Table 1. All these compounds exhibited notable antiviral activity, with EC_{50} values ranging from 0.002 μmol/L to 1.026 μmol/L. What is more, approximately half of the compounds demonstrated single-digit nanomolar activity against HIV-1 WT, especially compounds **11a**, **11e**, **11j**, **11p**–**11w**, and **11z**–**11ac**, which had greater potency than lead com-

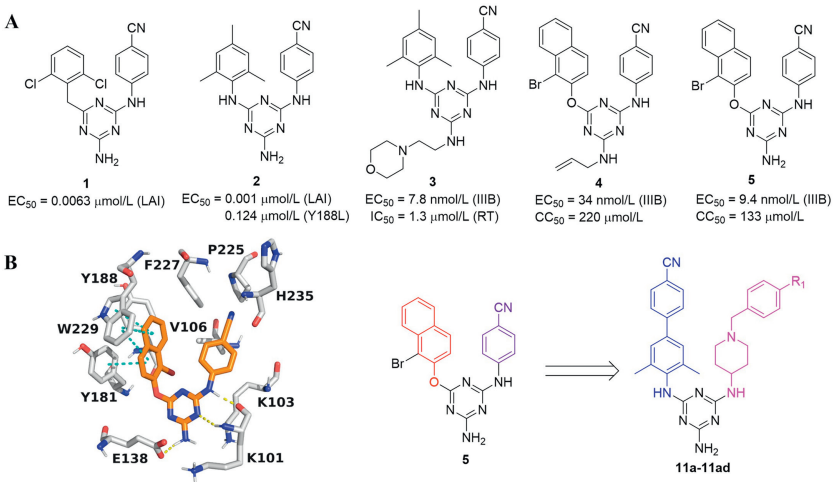
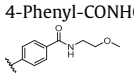
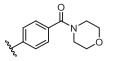
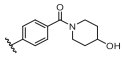
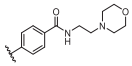
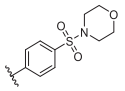


Fig. 1. (A) The chemical structures of triazines **1**–**5**. (B) The docking analysis of **5** (PDB code: 2zd1) and design of target compounds *via* rational structure-based drug design strategy.

Table 1
The anti-HIV-1 activity of **11a–11ad** against WT HIV-1 in MT-4 cells.

Compd.	R_1	EC_{50} (μmol/L)[a]	CC_{50} (μmol/L)[b]	SI[c]	Compd.	R_1	EC_{50} (μmol/L)	CC_{50} (μmol/L)	SI
11a	4-Phenyl-CN	0.008 ± 0.008	11.12 ± 1.64	1436	**11r**	4-Phenyl-SO_2CH_3	0.005 ± 0.001	4.98 ± 2.52	1027
11b	3-Phenyl-CN	0.080 ± 0.063	8.90 ± 1.20	111	**11s**	4-Phenyl-$CONH_2$	0.002 ± 0.001	19.69 ± 1.50	7438
11c	2-Phenyl-CN	0.040 ± 0.034	116.5 ± 6.07	2891	**11t**	3-Phenyl-$CONH_2$	0.006 ± 0.001	16.77 ± 2.52	2762
11d	4-Phenyl-F	0.009 ± 0.004	20.58 ± 9.57	2281	**11u**	4-Phenyl-$CONHCH_3$	0.008 ± 0.003	20.76 ± 3.63	2367
11e	4-Phenyl-Cl	0.008 ± 0.003	34.55 ± 11.24	4527	**11v**		0.004 ± 0.001	14.73 ± 2.28	3399
11f	4-Phenyl-CF_3	0.086 ± 0.072	107.9 ± 44.61	1255	**11w**		0.008 ± 0.003	17.99 ± 4.61	2291
11g	4-Phenyl-OCF_3	0.033 ± 0.013	>211.6	>6392	**11x**		0.018 ± 0.014	18.41 ± 1.53	998
11h	4-Phenyl-CH_3	0.300 ± 0.274	23.91 ± 6.18	80	**11y**		0.015 ± 0.011	16.18 ± 3.03	1107
11i	2,4-Phenyl-2-F	0.097 ± 0.086	8.86 ± 0.25	92	**11z**		0.008 ± 0.003	9.79 ± 10.53	1464
11j	3,4-Phenyl-2-F	0.008 ± 0.003	71.31 ± 8.42	8877	**11aa**	2-Pyridyl	0.006 ± 0.002	20.87 ± 3.04	3769
11k	4-Phenyl-COOH	0.223 ± 0.033	>227.8	>1021	**11ab**	3-Pyridyl	0.004 ± 0.002	18.83 ± 2.72	4759
11l	4-Phenyl-CH_2COOH	1.026 ± 0.226	209.7 ± 9.26	204	**11ac**	4-Pyridyl	0.003 ± 0.001	8.650 ± 2.870	3302
11m	4-Phenyl-$COOCH_3$	0.028 ± 0.012	52.23 ± 9.31	1872	**11ad**	2-Naphthyl	0.096 ± 0.139	83.83 ± 69.58	878
11n	3-Phenyl-COOH	1.014 ± 0.268	>227.8	>225	NVP	-	0.209 ± 0.091	>15.02	>72
11o	4-Phenyl-$B(OH)_2$	0.009 ± 0.004	14.51 ± 1.95	1569	EFV	-	0.004 ± 0.002	>6.34	>1425
11p	3-Phenyl-$B(OH)_2$	0.006 ± 0.002	13.36 ± 2.59	2166	ETR	-	0.003 ± 0.001	>4.59	>1340
11q	4-Phenyl-SO_2NH_2	0.008 ± 0.004	15.20 ± 2.33	1674					

[a] EC_{50}: concentration of compound required to achieve 50 % protection of MT-4 cell cultures against HIV-1-induced cytopathicity, as determined using the MTT method.
[b] CC_{50}: concentration required to reduce the viability of mock-infected cell cultures by 50 %, as determined using the MTT method.
[c] SI: the ratio of CC_{50}/EC_{50}.

pound **5** (EC_{50} = 0.002–0.008 *vs.* 0.009 μmol/L). Among them, compound **11s** emerged as the most outstanding one, boasting an EC_{50} value of 0.002 μmol/L, which surpassed not only the lead compound **5** but also the benchmark antiretroviral drugs NVP, EFV, and ETR (EC_{50} = 0.007, 0.209, 0.004, and 0.003 μmol/L, respectively). Moreover, **11s** (CC_{50} = 19.69 μmol/L) also showcased lower cytotoxicity than these drugs (NVP, CC_{50} > 15.02 μmol/L; EFV, CC_{50} > 6.38 μmol/L; ETR, CC_{50} > 4.59 μmol/L).

Preliminary investigations into the structure-activity relationships (SARs) have illuminated that the characteristics of substituents and their positions on the benzene ring play a pivotal role in determining antiviral activity. Generally, *para*-substituents are more favorable for enhancing antiviral activity compared to *ortho*- and *meta*-substituents (**11a** *vs.* **11b**–**11c**, **11k** *vs.* **11n**, **11s** *vs.* **11t**). In terms of electronic effects, electron-donating substituents, like the methyl group in compound **11h** (EC_{50} = 0.300 μmol/L), caused a marked reduction in anti-HIV-1 activity. In contrast, electron-withdrawing substituents in compounds **11a**–**11g** conferred relatively high anti-HIV-1 activity (EC_{50} = 0.008–0.086 μmol/L). Regarding multiple substitutions, double-substitution patterns, particularly at the 2,4-positions, did not lead to significant improvement in activity. For example, compound **11d** (EC_{50} = 0.009 μmol/L) showed higher activity than **11i** (EC_{50} = 0.097 μmol/L). The influence of the COOH group on antiviral activity was quite interesting. The presence of a COOH group alone led to a notable decrease in activity (**11k**, EC_{50} = 0.223 μmol/L). However, the effect could be modulated by the introduction of a methyl group. Inserting a methyl group between the COOH and the phenyl ring further diminished the activity (**11l**, EC_{50} = 1.026 μmol/L), while adding a CH_3 group at the end of the COOH group resulted in approximately a ten-fold increase in activity (**11m**, EC_{50} = 0.028 μmol/L).

Notably, the incorporation of other hydrophilic motifs significantly enhanced the antiviral activity (**11o**–**11t**, EC_{50} = 0.002–0.009 μmol/L). Among them, the order of their contribution to activity was $CONH_2$ > SO_2CH_3 > SO_2NH_2 > $B(OH)_2$. Subsequently, we modified the $CONH_2$ group with an array of diverse amino fragments. Although these derivatives were effective (**11u**–**11y**, EC_{50} = 0.004–0.018 μmol/L), none of them outperformed compound **11s**. Moreover, heterocyclic rings, specifically pyridyl substituents (**11aa**–**11ac**, EC_{50} = 0.003–0.006 μmol/L), were more advantageous than the 2-naphthyl group (**11ad**, EC_{50} = 0.096 μmol/L). In particular, **11ac** demonstrated potent antiviral activity (EC_{50} = 0.003 μmol/L), surpassing **5** and NVP, and being comparable to EFV and ETR.

Representative compounds **11p**, **11r**–**11t**, **11v**, and **11aa**–**11ac** were selected to evaluate their inhibitory potential against five mutant strains (L100I, K103N, Y181C, Y188L, and E138K). The corresponding results are presented in Table 2. Favorably, these chosen compounds exhibited a spectrum of inhibitory effects against the clinical mutants. Of particular note was their activity against the K103N mutant, which is the most commonly transmitted drug-resistant strain in clinical settings [2]. Among the tested compounds, compound **11s**, which had previously demonstrated the most potent activity against the WT strain, also displayed commendable anti-HIV-1 activity against the mutant strains. It achieved EC_{50} values of 0.021 μmol/L for the L100I mutant, 0.003 μmol/L for the K103N mutant, 0.013 μmol/L for the Y181C mutant, 0.073 μmol/L for the Y188L mutant, and 0.004 μmol/L for the E138K mutant. Significantly, **11s** exhibited greater potency against the Y181C and E138K mutations compared to the reference NVP and ETR. Furthermore, compounds **11r**, **11s**, **11v**, and **11ac** demonstrated single-digit nanomolar antiviral activity against the K103N mutation (EC_{50} = 0.003–0.005 μmol/L). In the case of the L100I and Y188L mutants, although **11s** and **11v** were slightly less potent than ETR, they also significantly exceeded NVP and EFV. Overall, these results offer promising prospects for the development of next-generation antiretroviral therapies with enhanced efficacy against both WT and mutant strains of HIV-1.

The inhibitory activity against WT HIV-1 RT enzymes of compounds **11a**–**11ad** was assessed and the data presented in Table

Table 2
The antiviral activity of selected compounds toward HIV-1 mutants.

Compd.	EC_{50} (μmol/L)[a]				
	L100I	K103N	Y181C	Y188L	E138K
11p	0.206 ± 0.145	0.020 ± 0.004	0.027 ± 0.007	0.304 ± 0.137	0.029 ± 0.015
11r	0.029 ± 0.012	0.005 ± 0.001	0.011 ± 0.002	0.157 ± 0.079	0.008 ± 0.002
11s	0.021 ± 0.090	0.003 ± 0.000	0.013 ± 0.003	0.073 ± 0.002	0.004 ± 0.001
11t	0.135 ± 0.060	0.024 ± 0.014	0.109 ± 0.080	0.513 ± 0.185	0.024 ± 0.019
11v	0.012 ± 0.004	0.005 ± 0.002	0.015 ± 0.005	0.068 ± 0.018	0.023 ± 0.018
11aa	0.174 ± 0.105	0.010 ± 0.003	0.036 ± 0.004	0.307 ± 0.080	0.011 ± 0.001
11ab	0.211 ± 0.076	0.012 ± 0.007	0.038 ± 0.017	0.545 ± 0.342	0.01 ± 0.003
11ac	0.046 ± 0.032	0.005 ± 0.003	0.011 ± 0.001	0.076 ± 0.006	0.011 ± 0.004
NVP	2.050 ± 1.896	5.197 ± 2.693	5.768 ± 2.976	> 15.02	0.157 ± 0.058
EFV	0.030 ± 0.015	0.084 ± 0.033	0.008 ± 0.003	12.67 ± 0.127	0.007 ± 0.003
ETR	0.007 ± 0.005	0.003 ± 0.001	0.016 ± 0.005	0.020 ± 0.008	0.009 ± 0.003

[a] EC_{50}: concentration of compound required to achieve 50 % protection of MT-4 cell cultures against HIV-1-induced cytopathicity, as determined using the MTT method.

S1 (Supporting information). Compounds **11a**–**11ad** displayed moderate RT inhibitory activity (IC_{50} = 0.20–1.70 μmol/L). Gratifyingly, approximately half of these compounds demonstrated superior inhibitory activity compared with NVP (IC_{50} = 0.75 μmol/L). Of particular significance, compounds **11s**, **11ab**, and **11ac** also emerged as the most potent inhibitors of RT. Notably, the RT inhibitory activity of **11ab** was 3.7-fold higher than that of NVP. These results suggest that compounds **11a**–**11ad** effectively target the RT enzyme.

To gain a deeper understanding of the binding mechanisms of compound **11s** with HIV-1 RT, molecular docking studies were carried out using Schrödinger Maestro 12.8. As depicted in Fig. 2A, compound **11s** was docked into the NNIBP, assuming a "horseshoe-shaped" conformation similar to that of the lead compound **5** and ETR. The biphenyl moiety of **11s** effectively inserted into the aromatic hydrophobic region and formed two π-π interactions with the Y181 and Y188 residues. These interactions not only enhanced the hydrophobic effect but also extended the length of the π-π stacking, thus validating the initial hypothesis regarding the design of the compound. At the core of the molecule, the N-1 position of the triazine ring participated in a water-mediated hydrogen bond with the E138 residue. Meanwhile, the adjacent NH group donated a hydrogen atom to form a crucial hydrogen bond with the backbone of the K101 residue. On the right wing, the piperidine linker acted as a bridge, positioning the terminal aryl motif within the groove surrounded by K104, V106, F227, and P236. Moreover, the protonated nitrogen atom of the piperidine formed a water-mediated bridge with the backbones of K103 and P236.

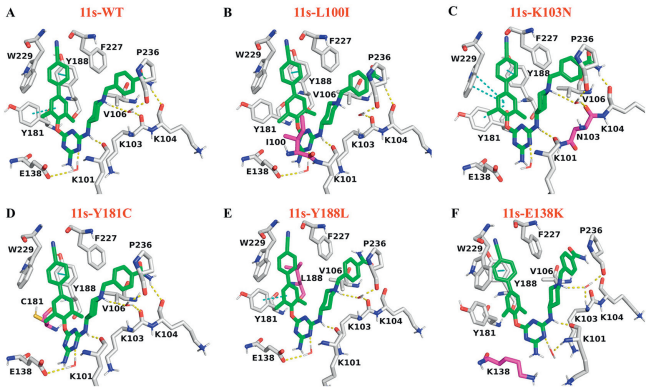


Fig. 2. The docking results of **11s** with HIV-1 RT. (A) **11s** with WT, (B) **11s** with L100I, (C) **11s** with K103N, (D) **11s** with Y181C, (E) **11s** with Y188L, and (F) **11s** with E138K. The protein carbon atoms were depicted in gray, mutant residues were depicted in purple and **11s** was presented in green. Dashed yellow lines represent the hydrogen-bonding interactions. Dashed pink lines represent the π-π interaction.

Additionally, the terminal $CONH_2$ substituent extended towards the solvent-exposed surface of the RT protein and formed an additional hydrogen bond with the backbone of K104. The binding model of **11s** with the mutant RT proteins was found to be highly similar to that with the WT RT. They all adopted the characteristic "horseshoe-shaped" conformations and maintained the crucial hydrogen bond interaction with the backbone of K101. In the cases of the L100I, Y181C, and Y188L mutants, the mutated residues led to the reduction or loss of one or more hydrogen bonds or π-π interactions with compound **11s**, which, in turn, resulted in a decrease in their antiviral efficacy. Notably, for the K103N mutant, although the water-mediated hydrogen bond between the N-1 position of the triazine ring and E138 was weakened, the dimethylphenyl moiety formed two additional π-π interactions with W229. These new interactions effectively compensated for the loss of the previous hydrogen bond. Intriguingly, the E138K mutation caused the loss of a water-bridge between **11s** and K138. However, a new water-mediated hydrogen bond was formed between **11s** and K101, offsetting the negative impact of the mutation.

The potent inhibition of cytochrome P450 (CYP) enzymes, particularly CYP2C9 and CYP2C19, by RPV and ETR has been well-documented, which leads to severe drug-drug interactions [7,38,39]. In light of these concerns, the inhibitory potential of compound **11s** against six major CYP isoforms was systematically evaluated. As presented in Table S2 (Supporting information), compound **11s** demonstrated negligible inhibitory activity against CYP1A2, CYP2D6, CYP3A4-M, and CYP3A4-T isoforms (IC_{50} > 50 μmol/L). Moreover, **11s** exerted only mild inhibitory effects on CYP2 sub-types. The IC_{50} values were determined to be 12.6 μmol/L for CYP2C9 and 14.7 μmol/L for CYP2C19. These values are significantly lower than those associated with ETR and RPV, suggesting that **11s** has a reduced propensity to interfere with the normal function of these CYP enzymes. Collectively, these findings indicate that compound **11s** presents a diminished risk of drug-drug interactions compared to RPV and ETR.

A significant number of drugs have been withdrawn from the market because of their high human ether-a-go-go-related gene (hERG) inhibitory activity [40]. RPV, for instance, has been linked to cardiotoxicity owing to its hERG-related side effects (IC_{50} = 0.50 μmol/L) [18]. Therefore, the hERG inhibitory activity of **11s** was evaluated and cisapride was used as a reference compound [41]. Encouragingly, compound **11s** exhibited a notably lower inhibitory effect on the hERG channel (IC_{50} = 15.979 μmol/L), which is substantially higher than those of cisapride and RPV (Fig. S1 in Supporting information). This outcome strongly suggests that compound **11s** poses a low risk of inducing cardiotoxic side effects.

Next, we evaluated metabolic stability of **11s** across five species. Table S3 (Supporting information) presents the metabolic stability data, which reveal a pronounced variation among the species

($t_{1/2}$ = 19.4–87.2 min). Notably, **11s** displayed the most extended $t_{1/2}$ (87.2 min) in mouse liver microsomes, accompanied by an exceptionally low intrinsic clearance rate (24 mL min^{-1} $gprot^{-1}$) and a commendable metabolic fraction (MF = 64.9 %). Even though the metabolic stability of **11s** in human and rat showed a slight decrease, the half-life and metabolic fractions remained more favorable compared to RPV ($t_{1/2}$ = 41.4 min, MF = 27.9 % (human); $t_{1/2}$ = 19.4 min, MF = 29.1 % (rat) *vs.* $t_{1/2}$ = 16.03 min, MF = 13.02 % (human); $t_{1/2}$ = 7.29 min, MF = 13.36 % (rat)) [42]. Collectively, these findings suggest that **11s** exhibits markedly enhanced metabolic stability, particularly when juxtaposed with the commercially available drug RPV.

Compound **11s** was proceeded to conduct pharmacokinetic (PK) studies in Sprague-Dawley rats using both single-dose intravenous (*i.v.*) and oral (*p.o.*) administrations (Table S4 in Supporting information). However, the half-life and oral bioavailability of compound **11s** remained poor ($t_{1/2}$ = 1.64 h, F = 1.52 %).

A single-dose acute toxicity study was carried out to comprehensively evaluate the *in vivo* safety profile of compound **11s**. Animal care and use protocols were approved by the Fudan University Committee on Animal Care (No. 2020CHEM-JS-009). As shown in Figs. S2A and B (Supporting information), there was neither mortality nor any significant alterations in body weight within the experimental group. This lack of adverse effects on survival and weight suggests that, at this dosage, **11s** does not induce immediate and obvious systemic toxicity. To further assess the potential impact of **11s** on vital organs, a histopathological examination was performed. The organs under scrutiny included the heart, liver, spleen, lungs, kidneys, and brain. Fig. S2C (Supporting information) presents the results of hematoxylin-eosin (HE) staining, a standard technique for visualizing tissue morphology. The staining results clearly demonstrated the absence of significant lesions or organ damage in the treated group. This indicates that **11s** does not cause detectable structural harm to these crucial organs at the tested dosage. Collectively, these findings provide strong evidence that compound **11s** is non-toxic at a dosage of 2000 mg/kg in mice.

In the ceaseless battle against the ever-evolving threat of HIV, the pursuit of more effective and safer antiretroviral agents remains a paramount objective. To this end, structure-based drug design strategy was rationally implemented, with the aim of augmenting the anti-resistance efficacy of the previously identified naphthyl-triazine compound **5**. This strategic initiative led to the rational design of a novel series of biphenyl-piperidine-triazine-containing NNRTIs. Several of these newly designed compounds demonstrated an extraordinary single-digit nanomolar antiviral potency against both the WT HIV-1 and five clinically relevant mutant strains. Among these compounds, **11s** emerged as a true champion. It exhibited unparalleled efficacy against WT HIV-1, with an EC_{50} value of 2 nmol/L, and also showed remarkable activity against the five mutant strains, with EC_{50} values ranging from 0.003 μmol/L to 0.073 μmol/L. These results are significantly superior to those of the lead compound **5**. When compared with the existing drugs ETR and RPV, compound **11s** achieved a 4-fold reduction in cytotoxicity. The metabolic profile of **11s** is equally impressive. It demonstrated exceptional stability, with an elimination half-life ($t_{1/2}$ = 41.4 min) more than double that of RPV ($t_{1/2}$ = 16.03 min). This extended half-life implies less frequent dosing, which can significantly improve patient compliance and the overall effectiveness of treatment. The comprehensive safety evaluation of **11s** further solidifies its potential as an antiretroviral agent. It showed minimal interference with CYP enzymes, low cardiac ion channel activity and no observable acute toxicity, suggesting a much lower risk profile for therapeutic applications. In conclusion, these promising characteristics of the biphenyl-piperidine-triazine derivatives, particularly compound **11s**, significantly elevate their development potential as next-generation NNRTIs. This not only provides new hope for HIV patients but also represents a major step forward in the global fight against this devastating disease.

Declaration of competing interest

The authors declare that they have no known competing financial interests or personal relationships that could have appeared to influence the work reported in this paper.

CRediT authorship contribution statement

Kun Zhang: Writing – original draft, Formal analysis, Data curation. **Li-Min Zhao:** Writing – original draft, Formal analysis, Data curation. **Tianhao Xing:** Writing – original draft, Data curation. **Yueyue Bu:** Writing – original draft, Data curation. **Qingyun Wang:** Writing – original draft, Data curation. **Christophe Pannecouque:** Writing – review & editing, Resources, Formal analysis. **Erik De Clercq:** Writing – review & editing, Project administration. **Angela Corona:** Writing – review & editing, Resources. **Laura Dettori:** Writing – original draft, Data curation. **Enzo Tramontano:** Writing – review & editing, Supervision. **Shuai Wang:** Writing – review & editing, Supervision, Project administration, Funding acquisition, Conceptualization. **Fen-Er Chen:** Writing – review & editing, Supervision, Conceptualization.

Acknowledgments

This work was financially supported by National Natural Science Foundation of China (No. 82304297) and the State Key Laboratory of Natural and Biomimetic Drugs (No. K202408).

Supplementary materials

Supplementary material associated with this article can be found, in the online version, at doi:10.1016/j.cclet.2025.111283.

References

[1] World Health Organization, HIV and AIDS (2024) https://www.who.int/news-room/fact-sheets/detail/hiv-aids.
[2] S. Gao, L. Song, Y. Cheng, et al., Acta Pharm. Sin. B 13 (2023) 2747–2764.
[3] K. Zhang, Y.J. Zhang, M. Li, et al., Med. Res. Rev. 45 (2024) 426–483.
[4] L. Zhao, C. Pannecouque, E. Clercq, et al., Acta Pharm. Sin. B 13 (2023) 4906–4917.
[5] D. Feng, H. Lin, L. Jiang, et al., Eur. J. Med. Chem. 246 (2023) 114957.
[6] X. Jin, S. Wang, L. Zhao, et al., Acta Pharm. Sin. B 13 (2023) 1192–1203.
[7] Y. Sang, C. Pannecouque, E. De Clercq, et al., Acta Pharm. Sin. B 13 (2023) 3054–3066.
[8] Q. Hao, X. Ling, C. Pannecouque, et al., Chin. Chem. Lett. 34 (2023) 107663.
[9] L. Zhao, C. Pannecouque, E. De Clercq, et al., Chin. Chem. Lett. 34 (2023) 108261.
[10] J. Ananworanich, B. Hirschel, Expert. Rev. Anti. Infect. Ther. 3 (2014) 51–60.
[11] T. Sibiya, T. Ghazi, A. Chuturgoon, Nutrients 14 (2022) 3076.
[12] R. Schrijvers, Expert. Opin. Pharmacother. 14 (2013) 1087–1096.
[13] A. Stockdale, S. Khoo, Curr. Opin. HIV. AIDS 17 (2022) 4–14.
[14] T. Lane, V. Makarov, J.A.E. Nelson, et al., J. Med. Chem. 66 (2023) 6193–6217.
[15] L. Ding, C. Zhuang, F. Chen, Med. Res. Rev. 41 (2021) 1255–1290.
[16] G. Li, Y. Wang, E. De Clercq, Acta Pharm. Sin. B 12 (2022) 1567–1590.
[17] Y. Sun, Z. Zhou, D. Feng, et al., J. Med. Chem. 65 (2022) 15608–15626.
[18] W. Huang, C. Pannecouque, E. De Clercq, et al., J. Med. Chem. 67 (2024) 19889–19904.
[19] D. Ludovici, R. Kavash, M. Kukla, et al., Bioorg. Med. Chem. Lett. 11 (2001) 2229–2234.
[20] B. Liu, Y. Lee, J. Zou, et al., Bioorg. Med. Chem. Lett. 20 (2010) 6592–6596.
[21] W. Lee, K. Frey, R. Gallardo-Macias, et al., Bioorg. Med. Chem. Lett. 25 (2015) 4824–4827.
[22] X. Chen, P. Zhan, X. Liu, et al., Bioorg. Med. Chem. 20 (2012) 3856–3864.
[23] W. Jorgensen, M. Bollini, V. Thakur, et al., J. Am. Chem. Soc. 133 (2011) 15686–15696.
[24] K. Jin, M. Liu, C. Zhuang, et al., Acta Pharm. Sin. B 10 (2020) 344–357.
[25] B. Viira, A. Selyutina, A.T. Garcia-Sosa, et al., Bioorg. Med. Chem. 24 (2016) 2519–2529.
[26] B. Huang, Z. Zhou, D. Kang, et al., Expert. Opin. Ther. Pat. 27 (2017) 9–15.
[27] X. Chen, Q. Meng, L. Qiu, et al., Chem. Biol. Drug. Des. 86 (2014) 122–128.
[28] Y. Xiong, H. Hu, F. Chen, et al., Acta Pharm. Sin. 44 (2009) 145–149.

[29] Y. Xiong, F. Chen, J. Balzarini, et al., Eur. J. Med. Chem. 43 (2008) 1230–1236.
[30] B. Meng, Z. Zhuo, H. Yu, et al., Chin. Chem. Lett. 35 (2024) 108827.
[31] D. Feng, F. Wei, Y. Sun, et al., Chin. Chem. Lett. 32 (2021) 4053–4057.
[32] S. Han, Y. Lei, C. Pannecouque, et al., Chin. Chem. Lett. 31 (2020) 764–768.
[33] Q. Deng, Q. Zheng, B. Zuo, et al., Green Synth. Catal. 1 (2020) 75–78.
[34] B. Gong, H. Zhu, Y. Liu, et al., Green Synth. Catal. 3 (2022) 110–115.
[35] J. Wang, K. Zhao, K. Zhang, et al., Bioorg. Chem. 147 (2024) 107340.
[36] K. Zhang, K. Hu, Q. Li, et al., J. Med. Chem. 66 (2023) 7221–7242.
[37] Y. Sang, C. Pannecouque, E. Clercq, et al., Bioorg. Chem. 111 (2021) 104905.
[38] Y. Sang, C. Pannecouque, E. Clercq, et al., Acta Pharm. Sin. B 13 (2023) 3054–3066.
[39] D. Kang, J. Yang, L. Kong, et al., Viruses 14 (2022) 2390.
[40] S. Kalyaanamoorthy, K.H. Barakat, Med. Res. Rev. 38 (2017) 525–555.
[41] S. Mohammad, Z. Zhou, Q. Gong, C.T. January, Am. J. Physiol. 273 (1997) H2534–H2538.
[42] W. Huang, C. Pannecouque, E. Clercq, et al., J. Med. Chem. 67 (2024) 17568–17584.